Journal Name

ARTICLE TYPE

Cite this: DOI: 00.0000/xxxxxxxxxx

Accelerating Dynamic Exchange and Self-Healing Using Mechanical Forces in Crosslinked Polymers

Nethmi De Alwis Watuthanthrige, a‡ Ballal Ahammed, b‡ Madison T. Dolan, a Qinghua Fang, b Jian Wu, c Jessica L. Sparks, d Mehdi B. Zanjani, b Dominik Konkolewicz, *a and Zhijiang Ye* b

Received Date Accepted Date

DOI: 00.0000/xxxxxxxxxx

Dynamically crosslinked polymers and their composites have tremendous potential in the development of the next round of advanced materials for aerospace, sensing, and tribological applications. These materials have self-healing properties, or the ability to recover from scratches and cuts. Applied forces can have a significant impact on the mechanical properties of nondynamic systems. However, the impact of force on the self-healing ability of dynamically bonded systems are still poorly understood. Here, we used a combined computational and experimental approach to study the impact of mechanical forces on the self-healing of a model dynamic covalent crosslinked polymer system. Surprisingly, the mechanical history of the materials has a distinct impact on the observed recovery in mechanical properties after the material is damaged. Higher compressive forces and sustained forces lead to greater self-healing, indicating that mechanical forces can promote dynamic chemistry. The atomistic details provided in molecular dynamics simulations are used to understand the mechanism with both non-covalent and dynamic covalent linkages responses to the external loading. Finite element analysis is performed to bridge the gap between experiments and simulations and to further explore the underlying mechanisms. The self-healing behavior of the crosslinking polymers is explained using the reaction rate theory. Overall, our study provides a fundamental understanding of how and why the self-healing of cross-linking polymers is affected by the compressive force and the force application time.

1 Introduction

Dynamically cross-linked polymers and their composites have tremendous potential in the development of the next generation of advanced materials. ^{1–4} These materials contain dynamic or exchangeable cross-linkers that fall into one of the following two categories: 1) non-covalent cross-linkers and 2) dynamic covalent cross-linkers. ^{5–12} Non-covalent cross-linkers are typically autonomically exchanging and display excellent self-healing and malleability properties. ¹³ However, these non-covalent bonds make the materials less tolerable towards the creep under applied stress. ¹³ In contrast, dynamic covalent linkages are strong and typically stimulus-responsive, allowing the resulting materials to be creep resistant. ¹⁴ Still, these materials are typically incapable

Up until now, many experimental oriented studies have been conducted on self-healing dynamically cross-linked polymers. Among them, intrinsic self-healing approaches have been developed for the polymeric materials with both reversible covalent, 20 and non-covalent bonds. 21 In addition, supramolecular polymers based on either hydrogen bonding, $\pi-\pi$ interactions, ionomers, and coordinative bonds have also been considered for the synthesis of self-healing polymers. $^{5,22-24}$ Similarly, many different types of dynamic covalent bonds have been incorporated into polymeric materials for self-healing type applications. $^{18,25-27}$ Among them, thiol-Michael adducts have shown excellent dynamic properties due to their facile bond formation through the "click"-like adduct forming reactions, 28 essentially static nature at room temperature, and bond activation by external stimuli such as heat or pH. 14,29,30

of self-healing until the substantial external stimulus is applied such as heat, pH, or light. ^{15–18} Additionally, materials containing dual dynamic cross-linking, where one linkage exchanges rapidly and provides autonomic dynamic character, while the other is a stimulus-responsive dynamic covalent linkage can further enhance self-healing performance in the material. ^{13,19}

^a Department of Chemistry and Biochemistry, Miami University, Oxford, OH 45056, USA. E-mail: konkold@miamioh.edu

 $[^]b$ Department of Mechanical and Manufacturing Engineering, Miami University, Oxford, OH 45056, USA. E-mail: zye@miamioh.edu

^c Department of Mechanical Engineering, Harbin Institute of Technology, China

^d Department of Chemical Paper and Biomedical Engineering, Miami University, Oxford, OH 45056, USA.

[‡] These authors contributed equally to this work.

In the computational aspect, theoretical models, molecular dynamics (MD) simulations, and Monte Carlo simulations have been used to investigate the self-healing behavior of polymers. Dementsov et al. investigated the self-healing composites using 3D numerical simulations within the percolation-model approach, reported that the competition between the healing capsules is more intense than in their earlier-explored 2D systems. 31 Ting Ge et al. studied the diffusion-based self-healing of polymer interfaces using the MD simulations. They showed that the diffusion across the interface is significantly faster in the damaged film compared to welding due to the presence of the short chains and the slow increment of interfacial strength of the healing film than the welding. 32 Yu et al. developed a theoretical model for dynamic crosslinked polymers to understand the self-healing and obtained consistence theoretical predictions with the experimental results.³³ Maiti et al. successfully captured the competition between reaction kinetics and crack propagation in self-healing polymers using cohesive modeling for crack propagation and coarse grain molecular dynamics. 34 Zheng et al. proposed a time-temperature superposition principle for a better understanding of the selfhealing mechanism.³⁵ In general, the self-healing process has been viewed as a transition from a non-equilibrium structure, where there are no crosslinks at the site of the damage, to an equilibrium state where the crosslink density is uniform throughout the material. ³⁶ The underlying mechanism of the mechanochemical behavior of self-healing polymers still requires further investigation. Further, Alsheghri et al. modeled the crack healing process of the materials using the cohesive zone framework and compared with the experimental results obtained with poly-methyl methacrylate (PMMA) samples. 37 They incorporated the effect of resting time, crack closure, and the history of healing and damage in the proposed cohesive zone model for a better understanding of the self-healing phenomena in the materials. However, this is for uncrosslinked and non-dynamically bonded PMMA materials. Qiu et al. investigated the self-healing behavior of bitumen pieces by pressing them against using a rheometer under a parallel-plate system. Concluding the main findings they figured out compressive forces have an effect on the time-dependent self-healing process of bitumen. 38 However, bitumen is a complex mixture of hydrocarbons and other components, and not a precisely engineered dynamic material. These two studies mainly focused on the effect of the external sources on the material self-healing properties but not the atomistic origin of the self-healing phenomena. Dynamic materials have unique bond exchange mechanisms to gain the self-healing ability within the materials.

In this study, we investigated the impact of the mechanical stimuli on the self-healing behavior of dynamically crosslinked polymers using combined experimental, MD simulation, and finite element approaches. This study combines experimental, simulation, and modeling data to probe the correlation between the self-healing process of dynamic covalent materials with the application of mechanical forces. Despite the stimulus-responsive nature of the thiol-Michael adducts and their essentially static properties at room temperature, ³⁹ a short period of mechanical compression under ambient temperature before thermal activation of the dynamic bonds can lead to substantial improvements

in the efficiency of self-healing. This is an unexpected result due to the lack of exchange of the dynamic bonds under the conditions where the mechanical force is applied. Theoretical approaches are used to rationalize the surprising observation.

2 Results and Discussion

Polymer materials (PEA_{100} - TM_6) were synthesized by RAFT polymerization using ethyl acrylate (EA) backbone, and 2-((ethoxycarbonothioyl)thio) ethyl acrylate (XEA) as the protected version of thiol cross linker. Primary chain lengths of 100 units with 6% thiol cross linker were synthesized. Figure S1 confirms that well-controlled polymers were synthesized, with number average molecular weight $M_n = 13000$ and molar mass dispersity of $M_w/M_n=1.16$. The polymers were cross linked using 1,1'-(Methylenedi-4,1-phenylene) bismaleimide to create the structure shown in Figure 1(a). The materials infrared spectrum is shown in Figure S2, with differential scanning calorimetry data in Figure S3 indicating that the materials have a glass transition near 0 °C, and are soft and elastomeric at or above ambient temperatures. These elastomeric properties are confirmed by rheological analysis, with Figure S4(a) showing frequency sweep data, suggesting the formation of a rubbery plateau, which is confirmed in the temperature sweep data in Figure S4(b). The molecular dynamics simulations were set up as described in Figure 1(b).

2.1 Mechanical Stability and Bond Exchange under Ambient Conditions

Creep deformation and creep recovery tests were performed to probe the dynamic bond exchange under ambient conditions. Highly dynamic materials exchange bonds under ambient conditions. This can cause these materials to display continuous creep deformation when constant stress applied at room temperature. If the bond exchange occurs on the timescale of the creep experiment, the materials will not return to their original shape once the stress is released. This is a major drawback of dynamically crosslinked materials in practical applications. As shown in figure 1(c), our dynamically crosslinked thiol-Michael materials attained mechanical equilibrium after 1 hour of constant applied force and stabilized for the next 3 hours without displaying further structural deformation. Dynamic covalent bonds usually activate and exchange under external stimuli such as heat or pH. However, the observed equilibration of this system suggests that, under the conditions applied, the exchanges between thiol-Michael dynamic bonds are insignificant and therefore the materials are resistant to continuous creep. Further, the long term creep recovery of these dynamically crosslinked materials were tested (figure 1(c) inset) after strained to 100% elongation for 24 hours. The material showed essentially full recovery to its original shape within one day. The thiol-Michael adducts within the polymer networks drive this creep recovery by maintaining the original network structure, which suggests negligible exchange. This is an important result since it shows that there is negligible bond exchange under ambient conditions, implying that the mechanical forces are applied under conditions where there is negligible bond exchange. To further confirm the importance of the

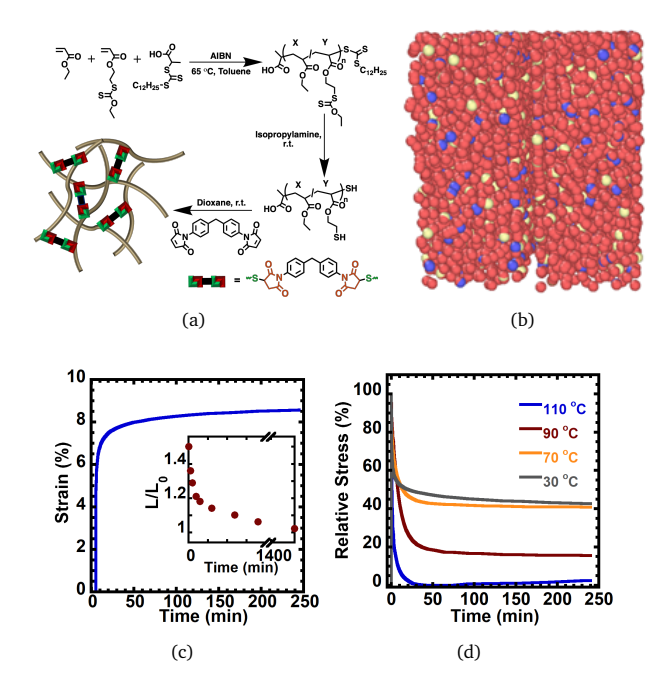


Fig. 1 (a) Synthesis of the polymer materials with dynamic thiol-maleimide linkages. Total monomers per chain on average: x=100; y=6; (Slashes indicate the random incorporation of monomers).(b) Illustration of the molecular dynamics simulation model, red beads represent the backbone monomers, yellow and red beads represent the crosslinkers. (c) Creep deformation of PEA_{100} - TM_6 materials as a function of time; Inset:Creep recovery of PEA_{100} - TM_6 material as a function of time, after the material was maintained at 100% for 24 hrs. (d) Stress relaxation of PEA_{100} - TM_6 materials as a function of time while the material was maintained at 3% strain at 110 o C, 90 o C, 70 o C, 30 o C for 4 hrs.

bond exchange in the studied materials, stress relaxation experiments were performed at different temperatures. At 30 o C there was a limited albeit rapid stress relaxation, which is attributed to the relaxation of the backbone units along the chains. This stress relaxation was limited by the essentially static nature of the thiol Michael adducts at room temperature. As shown in 1 (d), as the temperature increases, bond exchange occurs which increases the extent of stress relaxation at 90 o C, and eventually led to full relaxation at higher temperatures of 110 o C within 30 min.

2.2 Self-healing

In general, the self-healing process is driven towards the equilibrium by reforming the cross-linking across the boundary induced by the cut. The impact of the compressive mechanical force on self-healing was evaluated using two different approaches. In the first case, the same compressive force was used with the compression time varied. In the second case, the magnitude of the compressive forces was varied with a constant time over which the force is applied. In both cases, the compressive forces were applied to the cut surfaces by connecting the two cut pieces to the tensile testing instrument as shown in Figure S5(a). It is important to note that the compression time is in the order of seconds to minutes, while healing requires hours at elevated temperature. Figure 2(a) shows the impact of compression time with 0.5 N

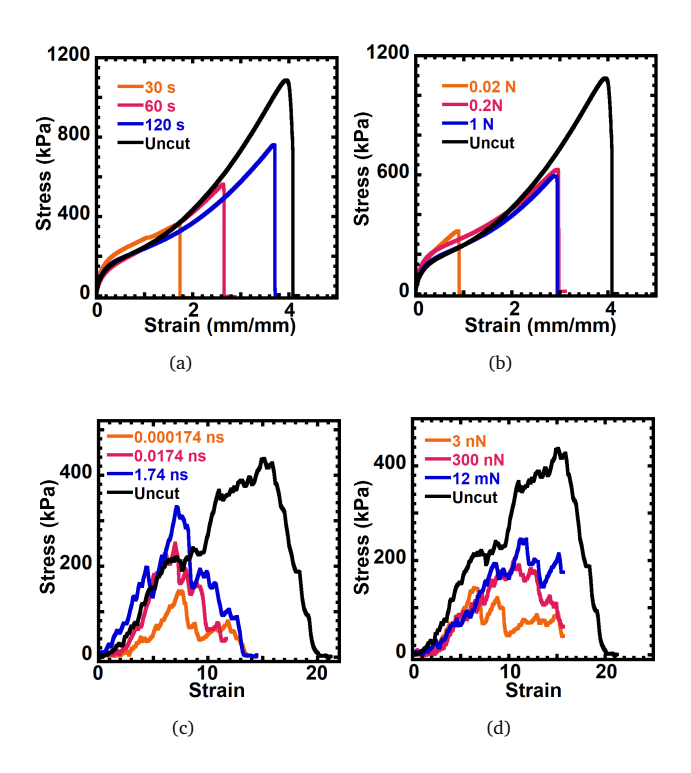


Fig. 2 Stress-strain curve for self-healing properties of the PEA_{100} - TM_6 materials (a) with different initial compressive force application time (b) with different initial compressive forces. Predicted stress-strain results from simulations with (c) initial compressive force application time and (d) with different initial compressive forces.

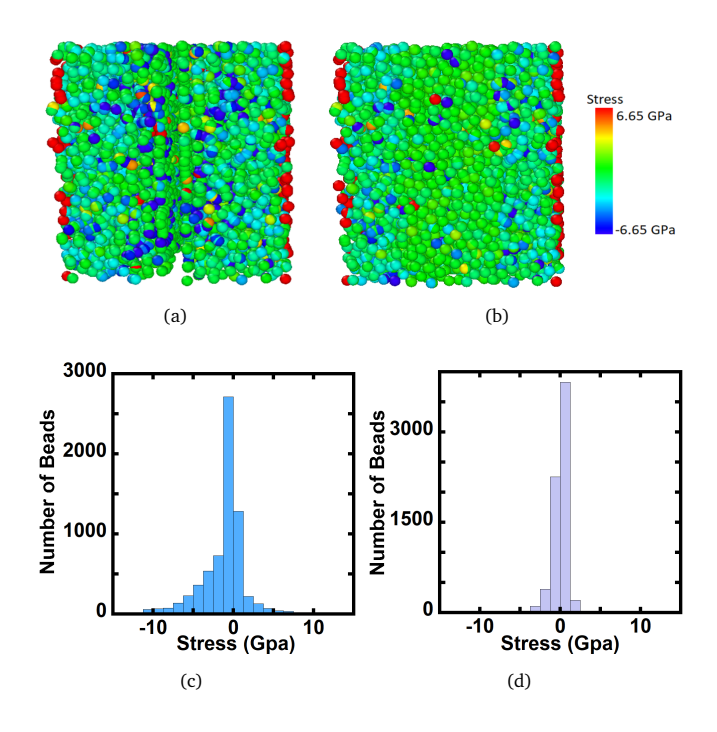


Fig. 3 Stress distribution of each atom of the polymer within the simulation domain (a) before and (b) after self-healing with the application of the compressive force prior to the healing time. Histogram of per-atom stress (c) before and (d) after self-healing.

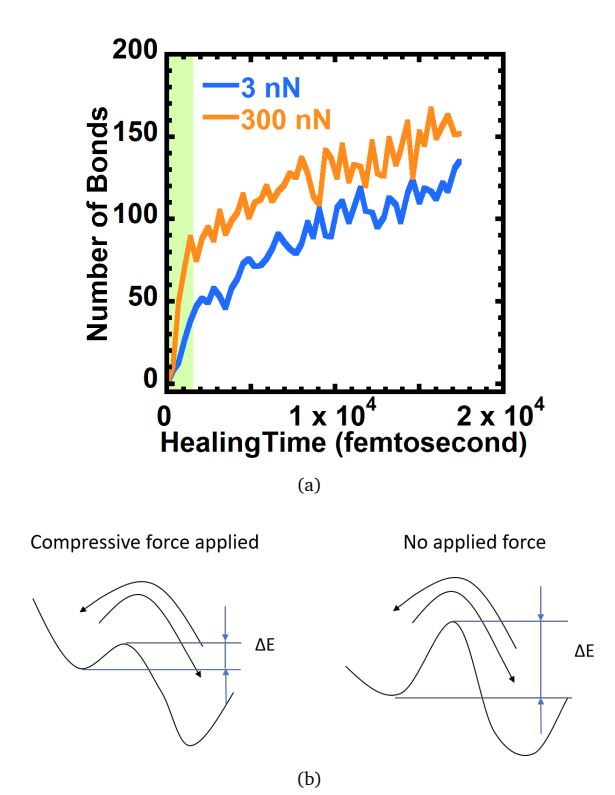


Fig. 4 (a) Bond formation during the self-healing process with different initial compressive force applied (in the highlighted time period). (b) Illustration of potential energy profile with and without compressive force applied.

applied force. Figure 2(a) gives experimentally measured stressstrain curves for a typical uncut material and cut samples that were subjected to 30, 60 and 120 s of 0.5 N compressive force prior to heating for 16 h at 90 °C to promote healing. The amount of self-healing is measured by the recovered maximum stress and strain. To determine if permanent changes in the material's mechanical properties were experienced during loading, compression analysis was performed on the cross linked materials both at 10% and 20% strain. Figure S6 indicates that no changes in the materials mechanical properties are seen as a result of these compressive forces through repeated loading analysis, even when the material is subjected to strain for a period of 60 s or 120 s. This implies that no net change in the material's mechanical properties is measurable as a result of the compressive forces applied. This could be because the uncut material is close to equilibrium both before and after the compression, implying that the compressive force made no net change to the structure. However, when there is a cut in the material, the structure is out of equilibrium as there are no linkages across the interface. Here, compressive forces could accelerate the progress towards an equilibrium structure, where the crosslink density is uniform across the whole material.

Figure 2(b) shows experimentally measured stress-strain responses for uncut and cut samples with the different compressive loads applied for 60 s. The cut samples were sliced in the middle with a razor and the two ends were compressed for 60 s under the different compressive loads of 0.02, 0.2, or 1 N. The experimental

data show that the self-healing efficiency increases with the compressive load applied, although this eventually reaches a plateau (Figure 2(b) and Figure S7(b)). Interestingly, self-healing efficiency increases with longer compressive force times and higher compressive forces, despite the fact that the thiol-Michael bonds are essentially static under the room temperature conditions used for the compression. Bond exchange should only occur upon thermal stimulus, which is after the compressive force has been applied and during the heating phase the material is not under compression. However, substantial improvements in self-healing are measured even with relatively short compressive times and relatively mild forces. This suggests that the compressive load can assist the reaction of crosslinkers by lowering the energy barriers. ⁴⁰

Both the external stimuli and compressive load play a vital role in self-healing studies. As shown in Figure S7, the application of heat can increase the dynamic bond exchange rate and provide better self-healing. Figure S7(a) shows that longer heating times lead to better self-healing. The compressive load establishes the contact between the cut surfaces and assist the bond exchange as well. However, we observed that without applying compressive load at the initial stage these materials fall apart even after 16 hours of heating time. Furthermore, to demonstrate the importance of the application of the external force, after the addition of initial compressive load, PEA100-TM6 materials were let to self-heal at RT. In this case, we could observe small selfhealing effect due to initially established contact between two cut surfaces through compression force and very slow exchange of thiol-Michael bonds at room temperature. Figure S7(b) indicates that the material which was compressed with 0.5 N but without heating showed substantially poorer self-healing than the material that was subjected to both compression and 16 h at 90 °C.

Figure 2(c) and (d) show the simulated stress-strain response for uncut and cut samples with different application times and magnitudes of the compressive force respectively. The simulation model was able to capture the experimental characteristic trends in self-healing with the applied compressive force prior to the healing time. Similar to the experimental results, self-healing was improved with both the magnitude and the application time of the compressive force. The magnitudes of the predicted stress and strain are different from experiments due to the difference between experimental and simulation conditions (size scale, time scale, etc). The strain values of our simulation model limit to a few hundreds of nanometers while the experimental conditions are on the millimeter scale. The simulation compressive time scale also significantly differs from the experimental values (from nanoseconds to seconds), due to the computational limitations. Other discrepancies between the model and experimental systems could be attributed to the presence of defects in the preparation of the materials. However, with the applied compressive force, only a maximum of 62% mechanical properties was recovered, even with long healing times. These results indicate that the intrinsic exchange is relatively slow, and the self-healing process may take an unreasonably long time to gain the full recovery of the mechanical properties. However, the application of the compressive force prior to the healing time helped to enhance the self-healing of dynamically crosslinked materials even with a short time period of compression. The effect of the force application time on self-healing can be explained by bond reaction process. ^{41,42} Yet, the mechanism underlying the observed enhancement of self-healing with the applied compressive forces requires further evidence and investigation. In order to understand and explain the underlying mechanisms, we employed molecular simulations to study the self-healing process with atomic-level details.

Figure 3(a) and (b) are color contour plots for stress distribution on each atom before and after self-healing with the application of the compressive force prior to the healing time. Our results indicate that the stress level of the atoms near the cut interface has significantly reduced after the self-healing process. Figure 3(c) and (d) are the corresponding histograms of the per-atom stress before and after self-healing. Before the process of selfhealing, the wide distribution of the histogram indicates the presence of a large number of atoms with high-stress values which are usually located near the cut interface. After the self-healing process, the distribution of the histogram narrowed down to a smaller range of stress values to evidence the presence of the fewer number of atoms under high-stress values. The differences in these stress distributions can be interpreted as the consumption of applied mechanical energy to drive the bond exchange reactions during the self-healing process, forming new cross-linking points across the interface.

Figure 4(a) shows the bond formation during the self-healing process with the application of different initial compressive forces. The force was applied on samples during the first 2000 femtoseconds and released afterword to mimic the experimental conditions and the formation of the bonds was observed for the later period of time. We observed an increased rate of the crosslink reformation with an increment of the number of bonds over time. Initially, a higher reaction rate (steeper slope) was observed for the system with the higher magnitude of the compressive force (300 nN load) compared with the other system (3 nN). However, after releasing the compressive force, both the systems displayed similar reaction rates for the reformation of bonds. The behavior of each system can be explained through the reaction rate theory. 43 In general, a reaction proceeds through a certain activation barrier (ΔE). The application of an initial compressive force (F_N) can affect the effective or apparent activation barrier and the rate of the forward reaction will proceed according to an Arrhenius relationship 40 as displayed in equation 1.

$$k_f = Ae^{-\frac{\Delta E(F_N)}{RT}} \tag{1}$$

Here, k_f is the reaction rate, A is the frequency factor, F_N is the applied load, R is gas constant, and T is temperature. As the applied load increases, the apparent energy barrier ΔE will be reduced. This is illustrated in Figure 4(b), and correspondingly the reaction rate k_f will increase. This explains why the reaction rate is significantly different when a different compressive force applied at the initial period of time, and also explains why the reaction rate is almost the same after the compressive force removed for both cases. This may even suggest that the compressive force is capable of activating dynamic bonds towards self-

healing, even under conditions that do not favor bond exchange, or that the compressive energy is retained under the healing conditions. Nevertheless, additional contributions to the enhanced self-healing after the compressive forces could also originate from improved contact and large contact are between the two surfaces upon compression or enhanced mixing at the interface. However, our combined experimental and simulation approach suggest that mechanically induced bond formation is likely to also contribute to the observed self-healing.

For the further bridging the gap between the experiments and MD simulations, we also performed a finite element analysis (FEA) to investigate this self-healing mechanism (details can be found in supplemental information SI). Our FEA model was able to capture the consistent trends with experiments and MD simulations in self-healing properties with the changes of the magnitude and the application time of the compressive force prior to the healing process (shown in Figure S8(a) and S8(b)). Agreement between the FEA model and experiments further validated the reliance of our FEA model. Figure S9(a) and S9(b) show the contour plots of stress distribution before and after self-healing. Higher stress was observed near the cut interface before the self-healing and it significantly reduced during self-healing which is consistent with our MD simulations prediction and further confirmed our hypothesis.

3 Conclusion

In this work, experiments, MD simulations, and finite element analysis were used to study the impact of the external mechanical forces on the self-healing in dynamically cross-linked polymers. Surprisingly, the application of the compressive forces prior to the thermal activation of the bonds leads to substantial improvements in self-healing properties even under the conditions that do not favor substantial bond exchange. For the first time, experiments, MD simulations, and finite element analysis were able to predict the same trends on self-healing properties of dynamic cross-linking polymers subjected to the initial compressive forces. The recovery of the mechanical stress and strain values during the self-healing process increased with the magnitude and the application time of the compressive force. MD simulations were able to provide the details of the atomic behavior on the stress distribution and bond formation during the self-healing process. Further, the effect of the compressive force was evaluated using the extracted stress, bond, and energy information through simulations. The mechanistic insights underlying the applied force was explained using the reaction rate theory. The application of a higher compressive force could change the potential energy profile of the reaction and subsequently reduce its activation energy barrier. A lower activation energy barrier can lead to a higher reaction rate according to the reaction rate model, and accelerate the bond formation and exchange in the dynamically cross-linked polymers. Overall, the results presented here provide an insight into how the self-healing of dynamically cross-linked polymers is affected by the magnitude and the application time of the compressive force and introduces mechanical force as a new tool to realize the exciting properties of dynamic materials.

Acknowledgements

B. Ahammed and N. De Alwis Watuthanthrige are equally contributed to this work. The authors acknowledge computational resources of the Ohio Supercomputer Center through Award PMIU0139. This material is based upon work supported by the National Science Foundation under Grant No. (DMR-1749730). Dominik Konkolewicz would also like to acknowledge support from the Robert H. and Nancy J. Blayney Professorship.

Notes and references

- H. Ma, A.-Y. Jen and L. R. Dalton, Advanced materials, 2002,
 14, 1339–1365.
- 2 A. Lendlein, M. Behl, B. Hiebl and C. Wischke, *Expert review of medical devices*, 2010, 7, 357–379.
- 3 W. F. Daniel, G. Xie, M. Vatankhah Varnoosfaderani, J. Burdynska, Q. Li, D. Nykypanchuk, O. Gang, K. Matyjaszewski and S. S. Sheiko, *Macromolecules*, 2017, **50**, 2103–2111.
- 4 H. Liang, S. S. Sheiko and A. V. Dobrynin, *Macromolecules*, 2018, **51**, 638–645.
- 5 F. Herbst, D. Döhler, P. Michael and W. H. Binder, *Macromolecular rapid communications*, 2013, **34**, 203–220.
- 6 M. Nakahata, Y. Takashima, H. Yamaguchi and A. Harada, *Nature communications*, 2011, **2**, 511.
- 7 M. Guo, L. M. Pitet, H. M. Wyss, M. Vos, P. Y. Dankers and E. Meijer, *Journal of the American Chemical Society*, 2014, **136**, 6969–6977.
- 8 X. Chen, M. A. Dam, K. Ono, A. Mal, H. Shen, S. R. Nutt, K. Sheran and F. Wudl, *Science*, 2002, **295**, 1698–1702.
- 9 M. Capelot, D. Montarnal, F. Tournilhac and L. Leibler, *Journal of the american chemical society*, 2012, **134**, 7664–7667.
- 10 X. Deng, R. Attalla, L. P. Sadowski, M. Chen, M. J. Majcher, I. Urosev, D.-C. Yin, P. R. Selvaganapathy, C. D. Filipe and T. Hoare, *Biomacromolecules*, 2017, 19, 62–70.
- 11 X. Yu, X. Chen, Q. Chai and N. Ayres, *Colloid and Polymer Science*, 2016, **294**, 59–68.
- 12 W. Zou, J. Dong, Y. Luo, Q. Zhao and T. Xie, *Advanced Materials*, 2017, **29**, 1606100.
- 13 B. Zhang, Z. A. Digby, J. A. Flum, E. M. Foster, J. L. Sparks and D. Konkolewicz, *Polymer Chemistry*, 2015, **6**, 7368–7372.
- 14 P. Chakma, Z. A. Digby, J. Via, M. P. Shulman, J. L. Sparks and D. Konkolewicz, *Polymer Chemistry*, 2018, **9**, 4744–4756.
- N. Roy, E. Buhler and J.-M. Lehn, *Polymer International*, 2014,
 63, 1400–1405.
- 16 J. J. Cash, T. Kubo, A. P. Bapat and B. S. Sumerlin, *Macromolecules*, 2015, **48**, 2098–2106.
- 17 K. Imato, A. Takahara and H. Otsuka, *Macromolecules*, 2015, **48**, 5632–5639.
- 18 P. Chakma and D. Konkolewicz, *Angewandte Chemie International Edition*, 2019, **58**, 9682–9695.
- 19 E. M. Foster, E. E. Lensmeyer, B. Zhang, P. Chakma, J. A. Flum, J. J. Via, J. L. Sparks and D. Konkolewicz, *ACS Macro Letters*, 2017, 6, 495–499.
- 20 Z. Wang and M. W. Urban, Polymer Chemistry, 2013, 4, 4897-

- 4901.
- 21 J. K. Hirschberg, L. Brunsveld, A. Ramzi, J. A. Vekemans, R. P. Sijbesma and E. Meijer, *Nature*, 2000, **407**, 167.
- 22 Z. P. Zhang, M. Z. Rong and M. Q. Zhang, *Progress in Polymer Science*, 2018, **80**, 39–93.
- 23 Z. Jiang, A. Bhaskaran, H. M. Aitken, I. C. Shackleford and L. A. Connal, *Macromolecular rapid communications*, 2019, 40, 1900038.
- 24 Z. Jiang, B. Diggle, I. C. Shackleford and L. A. Connal, *Advanced Materials*, 2019, **31**, 1904956.
- 25 L. Zhang, Z. Liu, X. Wu, Q. Guan, S. Chen, L. Sun, Y. Guo, S. Wang, J. Song, E. M. Jeffries et al., Advanced Materials, 2019, 31, 1901402.
- 26 D.-P. Wang, Z.-H. Zhao, C.-H. Li and J.-L. Zuo, *Materials Chemistry Frontiers*, 2019, **3**, 1411–1421.
- 27 D. Chen, Y. Zhang, C. Ni, C. Ma, J. Yin, H. Bai, Y. Luo, F. Huang, T. Xie and Q. Zhao, *Materials Horizons*, 2019, 6, 1013–1019.
- 28 D. P. Nair, M. Podgorski, S. Chatani, T. Gong, W. Xi, C. R. Fenoli and C. N. Bowman, *Chemistry of Materials*, 2013, **26**, 724–744.
- 29 B. Zhang, Z. A. Digby, J. A. Flum, P. Chakma, J. M. Saul, J. L. Sparks and D. Konkolewicz, *Macromolecules*, 2016, 49, 6871–6878.
- 30 P. Chakma, L. H. R. Possarle, Z. A. Digby, B. Zhang, J. L. Sparks and D. Konkolewicz, *Polymer Chemistry*, 2017, 8, 6534–6543.
- 31 A. Dementsov and V. Privman, *Physical Review E*, 2008, **78**, 021104.
- 32 T. Ge, M. O. Robbins, D. Perahia and G. S. Grest, *Physical Review E*, 2014, **90**, 012602.
- 33 K. Yu, A. Xin and Q. Wang, Journal of the Mechanics and Physics of Solids, 2018, 121, 409–431.
- 34 S. Maiti, C. Shankar, P. H. Geubelle and J. Kieffer, *Journal of Engineering Materials and Technology*, 2006, **128**, 595–602.
- 35 Z. Zheng, X. Xia, X. Zeng, X. Li, Y. Wu, J. Liu and L. Zhang, *Macromolecular rapid communications*, 2018, **39**, 1800382.
- 36 Y. Yang and M. W. Urban, *Healable Polymer Systems*, 2013, 126.
- 37 A. A. Alsheghri and R. K. A. Al-Rub, *Mechanics Research Communications*, 2015, **70**, 102–113.
- 38 J. Qiu, M. Van de Ven, S. Wu, J. Yu and A. Molenaar, *Fuel*, 2011, **90**, 2710–2720.
- 39 B. Zhang, P. Chakma, M. P. Shulman, J. Ke, Z. A. Digby and D. Konkolewicz, *Organic & biomolecular chemistry*, 2018, **16**, 2725–2734.
- 40 S. Raghuraman, M. Soleymaniha, Z. Ye and J. R. Felts, *Nanoscale*, 2018, **10**, 17912–17923.
- 41 E. B. Stukalin, L.-H. Cai, N. A. Kumar, L. Leibler and M. Rubinstein, *Macromolecules*, 2013, **46**, 7525–7541.
- 42 H. Yang, K. Yu, X. Mu, Y. Wei, Y. Guo and H. J. Qi, RSC Advances, 2016, **6**, 22476–22487.
- 43 P. Hänggi, P. Talkner and M. Borkovec, *Reviews of modern physics*, 1990, **62**, 251.